

# Effect of the beam-defocusing characteristics on porosity formation in laser welding

J. S. KIM\*, T. WATANABE\*\*, Y. YOSHIDA\*\*

\*Department of Precision & Production Engineering and \*\*Faculty of Engineering, Chiba University, 1-33, Yayoi-cho, Inage-ku, Chiba 263, Japan

Welding defects [1] are the principal factors that decrease the mechanical properties of welding construction. Porosities, which are one of the principal weld-defects, are formed in laser welding of light metals, such as Al alloys [1]. The porosities formed in high-power laser welding cause fracture of welding constructions due to decreased mechanical properties of the weld part. There are many reports about suppressing weld defects, but most of them are concerned with improvement of the welding structure, such as generation of cracks and micro-crystallization [2-5]. On the other hand, there are very few reports about suppressing the formation of porosities [5-6], because the mechanism of porosity formation is not clear. However, when the proposed mechanism of porosity formation is considered, the formation of porosities can be suppressed by providing ultrasonic vibration to the molten pool during laser welding [6]. However, this welding method is unable to suppress completely porosity formation during high-power laser welding.

Therefore, the suppression limit of porosity formation is investigated in this paper. Namely, the optimum beam-defocusing condition for suppressing porosity formation is determined in high-power laser welding of Al alloys by consideration of beam-defocusing characteristics due to the wall-focusing effect. Moreover, at the same time the relation of the defocus value to the geometrical features of molten zones and porosity formation rate are also investigated.

Materials used in this experiment were A1050 (99.12% Al) and A6061 (0.4-0.8% Si, 0.8-1.2% Mg, 0.7% Fe, 0.25% Zn).

The laser operation mode used in this experiment was a normal pulsed Nd:YAG laser. Pulse durations of the laser output waveform were 5 ms and 9 ms.

Laser spot welding without a filler metal was carried out. The cross-sections of spot-welded part were polished, treated with electrolytic polishing and finally etched. The geometrical characteristics of the molten zones, aspect ratio and porosity formation rate were investigated on cross-sections of the melt.

Al alloys are characterized by good properties such as high strength-to-weight ratio, good mechanical properties, good workability and high corrosion resistance. But, the effective weldability of Al alloys is very poor because of high reflectivity and thermal conductivity.

However, absorptivity of aluminum increases

from less than 10% at room temperature to 40-50% at its melting point, and to as high as 90% at its vaporization point [7]. Thus, control of laser energy density is difficult in laser welding in keyhole mode since the focal point approaches the keyhole bottom. Thus the excessive pressure generated in the keyhole is relieved by adequate control of the defocus value. Then a decreased porosity formation rate can be presumed.

Fig. 1 shows the phenomenon of beam transition [8] from thermal-conductive mode (i.e. shallow penetration) to keyhole mode (i.e. deep penetration) welding.

Only the limiting trace rays are shown in this figure.

When the laser energy density exceeds a certain limit in the transition from thermal-conductive mode to keyhole mode, the reaction force of the evaporated metal gas increases rapidly. Vibration and deformation of the liquid surface becomes large due to the increased vapour pressure. Then a keyhole is formed in the molten pool, and the material is heated directly by the laser beam through the keyhole. Thus deep-penetration welding by the keyhole mode is achieved. When the focal point is set into the material (see Fig. 1;  $def. < 0$ , O-C

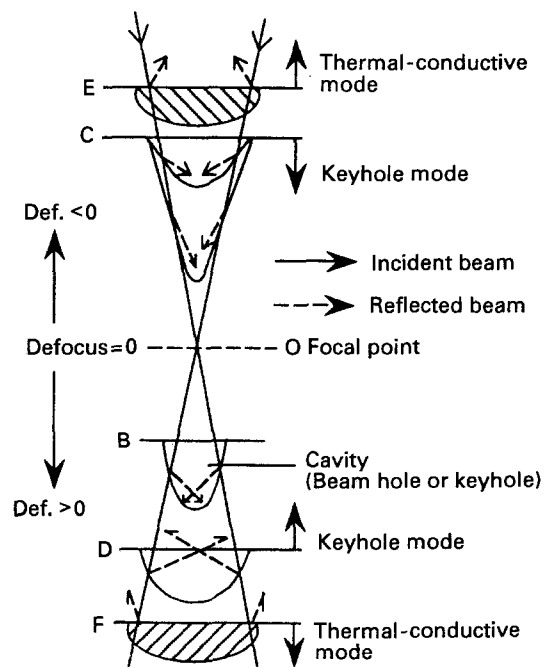


Figure 1 Schematic diagram of change of welding mode from thermal-conductive mode to keyhole mode.

zone), the reflected beam loss is decreased by multiple reflections at the keyhole wall. At the same time, the increase in the power density at the bottom of the keyhole is enhanced by a wall-focusing effect, which is caused by refocusing the beam reflected from the keyhole wall. Also, the increase in keyhole depth leads to an increased number of reflections, thereby increasing the beam power at the bottom of the keyhole: this rapidly generates excessive pressure at the bottom of the keyhole. Therefore, temporal fluctuation and spatial instability of the keyhole are induced. The incident beam proceeds to the bottom of the keyhole through multiple reflections. Furthermore the absorptivity increases rapidly by generation of the keyhole, through which the increment of vapour pressure is also promoted rapidly by the beam concentrated at the bottom of the keyhole. Moreover, the defocus value depends upon the quantity of light elements such as Mg or Zn having a low vaporization point as well as high vapour pressure. At this time, the porosities are easily formed by the collapse of the balance of force acting on the keyhole. Therefore it is necessary to select the adequate defocused value in order to decrease the beam-concentration effect at the bottom of the keyhole by multiple reflections as shown in Fig. 1.

When the penetration depth is constant, the typical shapes of molten zones as a result of changes of the defocus value are shown in Fig. 2.

When the defocus value increases, considerable incident energy is required in order to obtain a constant depth of penetration. On the other hand, a stable shape of molten zone is obtained. Moreover, at near focal point (*def.* = -1, 0 and +1 mm), sharp-shaped molten zones with many irregular porosities are observed. These results suggest that the effect of beam concentration at the point of the keyhole is bead transition.

Figs 3 and 4 indicate the relationship between aspect ratio and porosity formation rate when the defocus value is more than  $\pm 2$  mm. These figures show the results of porosity formation rate for aluminium (A1050) and Al alloy (A6061), respectively.

Generally, porosity formation rate increased with increase of aspect ratio. Moreover, the difference of

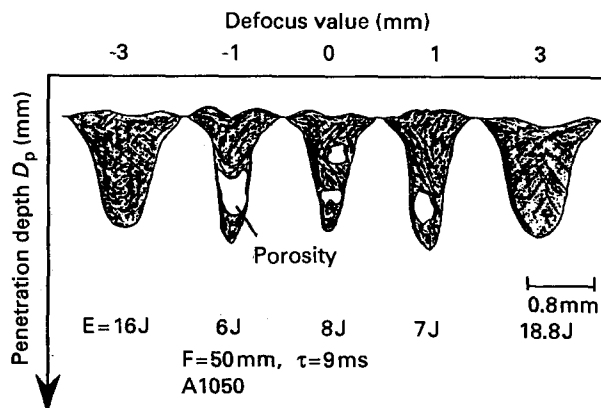


Figure 2 Schematic cross-sections of laser-spot molten zones for aluminium (A1050).

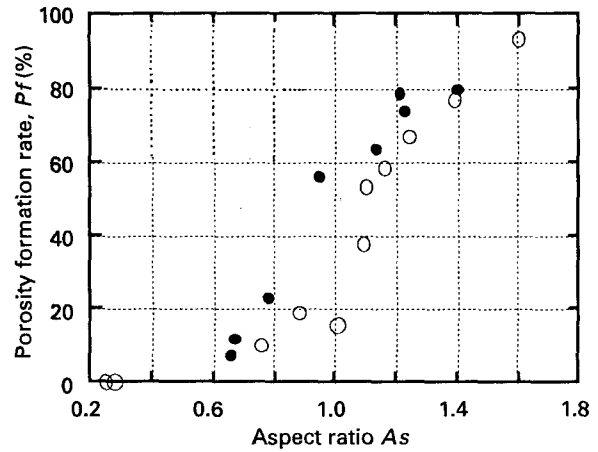


Figure 3 Relationship between aspect ratio and porosity formation rate (A1050).  $F = 50$  mm,  $\tau = 9$  ms.  $\circ$  PF (*def.* = +);  $\bullet$  PF (*def.* = -).

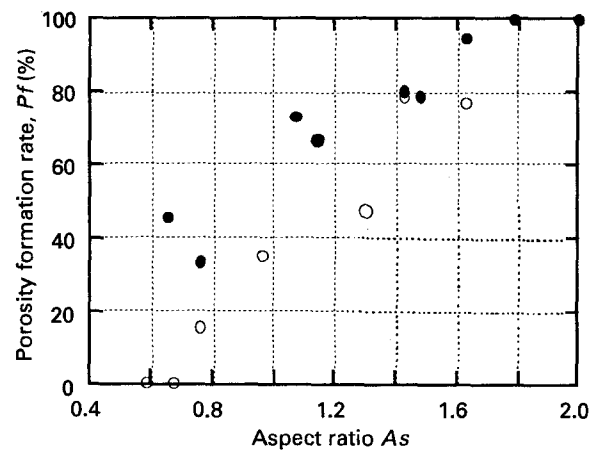


Figure 4 Relationship between aspect ratio and porosity formation rate (A6061).  $F = 50$  mm,  $\tau = 9$  ms.  $\circ$  PF (*def.* = +);  $\bullet$  PF (*def.* = -).

porosity formation rate for positive and negative defocus values is small for A1050 aluminium, but this difference is large for A6061 Al alloy. These results suggest that the defocus value depends on the contents of light elements such as Mg or Zn. When the penetration depth is set at constant value ( $D_p = 1.5$  mm), the effects of defocus value on the porosity formation rate are obtained, as shown in

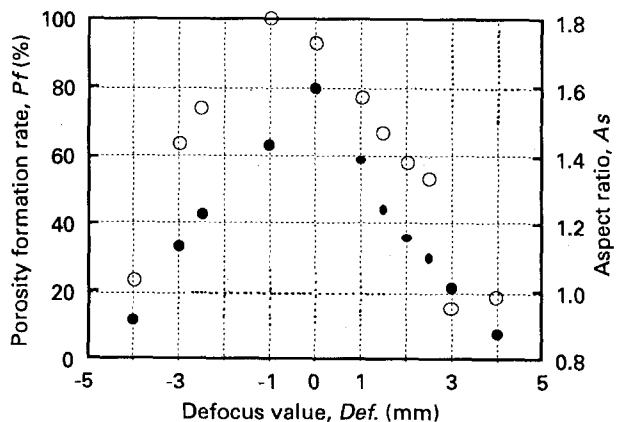


Figure 5 Effect of defocus value on porosity formation rate at constant penetration depth (A1050).  $F = 50$  mm,  $\tau = 9$  ms,  $D_p = 1.5$  mm.  $\circ$  PF;  $\bullet$  As.

Fig. 5. The aspect ratio and the porosity formation rate increase as the defocus value approaches zero. Porosity formation can be suppressed by adequate defocus values of  $def. = -4$  mm and  $def. = +3$  mm (Fig. 5).

In conclusion, the porosity formation rate decreased by about five times by controlling the defocus value. The optimum defocus values obtained in these experiments were: above  $def. = +3$  mm; and below  $def. = -4$  mm. Needless to say, the optimum defocused value was dependent on the chemical composition of the materials.

### Acknowledgement

The authors wish to express appreciation to Mr N. Hagiwara for his cooperation in this work.

### References

1. A. SAKAGUCHI, Y. TOMII and M. MIZUNO, *J. Jpn Inst. Light Metals* **21** (1983) 547.
2. R. H. PHILLIPS and E. A. METZBOWER, *Welding J.* June (1992) 201.
3. M. J. CIESLAK and P. W. FUERSCHBACK, *Metallurgical Trans. B* **19B** (1988) 319.
4. S. KATAYAMA and C. D. LUNDIN, *J. Light Metal. Welding and Construction* **29** (1991) 349.
5. A. MATSUNAWA, S. KATAYAMA, H. IKEDA and K. NISHIZAWA, *Int. Congress on Applications of Laser and Electro-optics*, **75** (1992) 547.
6. J. S. KIM, T. WATANABE and Y. YOSHIDA, *J Laser Applic* **7** (1995) 38.
7. S. L. ENGEL, *American Machinist*, May (1976) 107.
8. I. MIYAMOTO, H. MARUO and Y. ARATA, *Proceedings of International Conference on Welding Research*, A18 (1980) 103.

*Received 13 October 1994*

*and accepted 17 January 1995*